



# Microheater Array Boiling Experiment

Jungho Kim  
University of Maryland, College Park, Maryland

John McQuillen and Joe Balombin  
Glenn Research Center, Cleveland, Ohio

## The NASA STI Program Office . . . in Profile

Since its founding, NASA has been dedicated to the advancement of aeronautics and space science. The NASA Scientific and Technical Information (STI) Program Office plays a key part in helping NASA maintain this important role.

The NASA STI Program Office is operated by Langley Research Center, the Lead Center for NASA's scientific and technical information. The NASA STI Program Office provides access to the NASA STI Database, the largest collection of aeronautical and space science STI in the world. The Program Office is also NASA's institutional mechanism for disseminating the results of its research and development activities. These results are published by NASA in the NASA STI Report Series, which includes the following report types:

- **TECHNICAL PUBLICATION.** Reports of completed research or a major significant phase of research that present the results of NASA programs and include extensive data or theoretical analysis. Includes compilations of significant scientific and technical data and information deemed to be of continuing reference value. NASA's counterpart of peer-reviewed formal professional papers but has less stringent limitations on manuscript length and extent of graphic presentations.
- **TECHNICAL MEMORANDUM.** Scientific and technical findings that are preliminary or of specialized interest, e.g., quick release reports, working papers, and bibliographies that contain minimal annotation. Does not contain extensive analysis.
- **CONTRACTOR REPORT.** Scientific and technical findings by NASA-sponsored contractors and grantees.

- **CONFERENCE PUBLICATION.** Collected papers from scientific and technical conferences, symposia, seminars, or other meetings sponsored or cosponsored by NASA.
- **SPECIAL PUBLICATION.** Scientific, technical, or historical information from NASA programs, projects, and missions, often concerned with subjects having substantial public interest.
- **TECHNICAL TRANSLATION.** English-language translations of foreign scientific and technical material pertinent to NASA's mission.

Specialized services that complement the STI Program Office's diverse offerings include creating custom thesauri, building customized data bases, organizing and publishing research results . . . even providing videos.

For more information about the NASA STI Program Office, see the following:

- Access the NASA STI Program Home Page at <http://www.sti.nasa.gov>
- E-mail your question via the Internet to [help@sti.nasa.gov](mailto:help@sti.nasa.gov)
- Fax your question to the NASA Access Help Desk at 301-621-0134
- Telephone the NASA Access Help Desk at 301-621-0390
- Write to:  
NASA Access Help Desk  
NASA Center for Aerospace Information  
7121 Standard Drive  
Hanover, MD 21076



# Microheater Array Boiling Experiment

Jungho Kim  
University of Maryland, College Park, Maryland

John McQuillen and Joe Balombin  
Glenn Research Center, Cleveland, Ohio

Prepared for the  
International Space Station Utilization—2001  
sponsored by the American Institute of Aeronautics and Astronautics  
Cape Canaveral, Florida, October 15–18, 2001

National Aeronautics and  
Space Administration

Glenn Research Center

Available from

NASA Center for Aerospace Information  
7121 Standard Drive  
Hanover, MD 21076

National Technical Information Service  
5285 Port Royal Road  
Springfield, VA 22100

Available electronically at <http://gltrs.grc.nasa.gov/GLTRS>

# MICROHEATER ARRAY BOILING EXPERIMENT

Jungho Kim  
University of Maryland  
College Park, Maryland 20742

John McQuillen and Joe Balombin  
National Aeronautics and Space Administration  
Glenn Research Center  
Cleveland, Ohio 44135

## ABSTRACT

Pool boiling in microgravity is an area of both scientific and practical interest. By conducting tests in microgravity as well as lunar and Martian gravity, it is possible to assess the effect of buoyancy on the overall boiling process and assess the relative magnitude of effects with regards to other "forces" and phenomena such as Marangoni forces, liquid momentum forces, and microlayer evaporation.

Two experimental packages have been designed, built and tested on the KC-135 and a Terrier Orion Sounding Rocket. Preliminary data reduction indicates that there is little effect of gravity on boiling heat transfer at wall superheats below 25 °C, even though there were vast differences in bubble behavior between gravity levels. At all superheats in microgravity, a large primary bubble moved over the surface, occasionally causing nucleation to occur. This primary bubble was surrounded by smaller satellite bubbles. Once formed, the primary bubble's size remains constant for a given superheat, indicating a balance between evaporation at the bubble base and condensation on the bubble cap. The size of the primary bubble increased with increasing wall superheat. Most of the heaters under the primary bubble indicated low heat transfer, suggesting that dryout occurred on the heater surface. Strong Marangoni convection around the bubble was observed to develop in microgravity, forming a "jet" of fluid into the bulk liquid. This "jet" also provided a reaction force on the primary bubble, and kept the bubble on the heater. At a superheat of 30 °C, the microgravity data fell significantly below the 1 g and 1.8 g data due to a large part of the heater surface drying out.

An experiment is now being designed for the Microgravity Science Glovebox that will extend the range of test conditions to include longer test durations

and less liquid subcooling. The objective is to determine the differences in local boiling heat transfer mechanisms in microgravity and normal gravity from nucleate boiling, through critical heat flux and into the transition boiling regime

This experiment will use two 96 element microheater arrays, 2.7 and 7.0 mm in size. These heaters are individually controlled to operate at a constant temperature, allowing local heat fluxes to be measured as a function of time and space. Most boiling experiments in the past have operated at constant wall heat flux with a much larger heater, allowing only time and space-averaged measurements to be made. Each heater is on the order of the bubble departure size in normal gravity, but significantly smaller than the bubble departure size in reduced gravity.

## INTRODUCTION

Boiling is a complex phase transition process where the physics of hydrodynamics, heat transfer, mass transfer, and interfacial phenomena are tightly interwoven. It is of importance to space-based hardware and processes such as heat exchangers, cryogenic fuel storage and transportation, electronic cooling, and material processing due to the large amounts of heat that can be removed with relatively little increase in the temperature of the heat transfer fluid. An understanding of boiling and critical heat flux in reduced gravity environments (lunar, Martian, and microgravity) is important to the design of future heat removal equipment for these space-based applications.

Although much research in this area has been performed since the Space Station was proposed, the various mechanisms by which heat is removed from surfaces and their relative importance are still unclear. It is generally thought that heat removed from a surface

by single bubbles during nucleate boiling follows a sequence of events. Before bubble nucleation, heat is transferred from the wall to the fluid by natural convection (provided that there is a sufficient gravity level to generate a buoyancy driven flow) and heat conduction through the growing thermal boundary layer. Once a bubble is formed, various heat transfer mechanisms are possible (see Figure 1) including the following: conduction heat transfer ( $Q_{\text{liquid conduction}}$ ) and natural convection from the heated wall to the fluid ( $Q_{\text{natural convection}}$ ), conduction through the vapor layer ( $Q_{\text{vapor}}$ ), conduction and evaporation through the liquid microlayer ( $Q_{\text{microlayer}}$ ), evaporation of liquid due to the superheated liquid layer ( $Q_{\text{evaporation}}$ ), and Marangoni (surface tension) convection ( $Q_{\text{Marangoni}}$ ). Of the above mechanisms, it is thought that  $Q_{\text{evaporation}}$  and  $Q_{\text{microlayer}}$  play dominant roles in the heat transfer process. When the bubble departs from the surface (due to buoyancy forces in gravity or through inertia forces in microgravity), a vortex ring behind the departing bubble is generated which drags the superheated liquid layer away from the heater and replaces it with a new layer of cold liquid.<sup>2</sup>

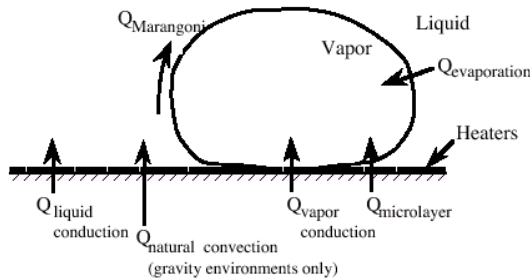


**Figure 1: Heat transfer mechanisms in nucleate boiling.**

The cycle then repeats. In earth gravity, natural convection and buoyancy are the dominating mechanisms that affect the boiling heat transfer by governing the rate at which bubbles leave the heater surface. A simple model describing the bubble departure size can be obtained by balancing the buoyancy force trying to lift the bubble against the and surface tension that holds the bubble to heater and is given by the Fritz<sup>1</sup> relation:

$$\sqrt{Bo} = 0.208 \cos \theta \quad (1)$$

where  $\theta$  is the contact angle in degrees and  $Bo$  is the bond number. For small, rapidly growing bubbles, the inertia associated with pushing the liquid out of the way of the growing bubble can also cause bubble departure. In microgravity, the magnitude of effects related to natural convection and buoyancy are small and physical

mechanisms normally masked by natural convection in earth gravity such as Marangoni convection can substantially influence boiling and vapor bubble dynamics in microgravity. CHF is also substantially affected by microgravity.

In normal gravity environments,  $Bo$  has been used as a correlating parameter for CHF. Zuber's<sup>9</sup> CHF model for an infinite horizontal surface assumes that vapor columns formed by the merger of bubbles become unstable due to a Helmholtz instability blocking the supply of liquid to the surface. The jets are spaced  $\lambda_D$  (the Taylor wavelength) apart, where

$$\lambda_D = \frac{2\pi\sqrt{3}}{\sqrt{Bo}} = \sqrt{3}\lambda_c \quad (2)$$

and is the wavelength that amplifies most rapidly. The critical wavelength  $\lambda_c$  is the wavelength below which a vapor layer underneath a liquid layer is stable. For heaters with  $Bo$  smaller than about 3 (heaters smaller than  $\lambda_D$ ), this model is not applicable, and surface tension effects dominate. Bubble coalescence is thought to be the mechanism for CHF under these conditions. Small  $Bo$  can result by using smaller heater sizes in normal gravity, or by operating a large heater in a lower gravity environment. In microgravity, even large heaters can have low  $Bo$ , and models based on Taylor and Helmholtz instabilities should not be applicable. The macrolayer model of Haramura and Katto<sup>3</sup> is dimensionally equivalent to Zuber's<sup>9</sup> model, so it should not be applicable as well.

The overarching goal of this work is to determine how boiling heat transfer mechanisms for a flat plate in microgravity are altered from those in earth gravity. It is hypothesized that coalescence becomes the primary bubble removal mechanism in microgravity, and causes the formation of a large "primary" bubble. If this bubble is attached to the surface, it causes local dryout to occur, and heat can only be transferred from the surface by the smaller bubbles surrounding the primary bubble. This small-scale boiling behavior is similar across gravity levels, and it is hypothesized that boiling curves in microgravity can be obtained from knowledge of earth gravity data and the size of the primary bubble in microgravity.

#### EXPERIMENTAL APPROACH

Most boiling and heat transfer studies utilize a constant heat flux approach whereby power into the heater is supplied at a constant rate. Local temperature measurements can be made, but generally are limited to a few discrete sites, although thermal imaging and

temperature sensitive paints are now utilized to give a more complete picture. While constant heat flux techniques are typically easy to implement experimentally, data analysis must not only account for heat loss through the heater substrate to the backside, but also for temperature variations within the heater surface due to the boiling process. Dryout of the liquid film on the wall will cause the temperature to rise in that location, while the temperature is lower where there is liquid contact. Because the local temperatures must increase significantly, burnout or premature heater failure occurs as the material properties of the heater are eventually compromised at elevated temperatures.

For this experiment, the local surface heat flux measurements and constant temperature control are provided by an array of ninety-six platinum resistance heaters deposited on a quartz wafer. A photograph of boiling on this heater array taken through the quartz substrate is shown in Figure 2. Each of the individual heaters in the Figure is about 0.26 by 0.26 mm in size, has a nominal resistance of 1000 and a nominal temperature coefficient of resistance of  $0.002\text{ }^{\circ}\text{C}^{-1}$ . Up to 17 heater arrays can be fabricated simultaneously on a single quartz wafer using VLSI circuit fabrication techniques. Platinum is sputtered onto the entire surface of a  $500\text{ }\mu\text{m}$  thick wafer to a thickness of  $0.2\text{ }\mu\text{m}$ , a layer of photoresist is deposited and patterned to define the heater geometry. The platinum from the un-masked areas is removed using an ion mill to form a resistance heater. The platinum lines within each individual heater are  $5\text{ }\mu\text{m}$  wide and spaced  $5\text{ }\mu\text{m}$  apart. Aluminum is then vapor-deposited to a thickness of  $1\text{ }\mu\text{m}$  onto the surface, the aluminum power leads are masked off, and the remaining aluminum is removed using a wet chemical etch. A layer of  $\text{SiO}_2$  is finally deposited over the heater array to provide the surface with a uniform surface energy.

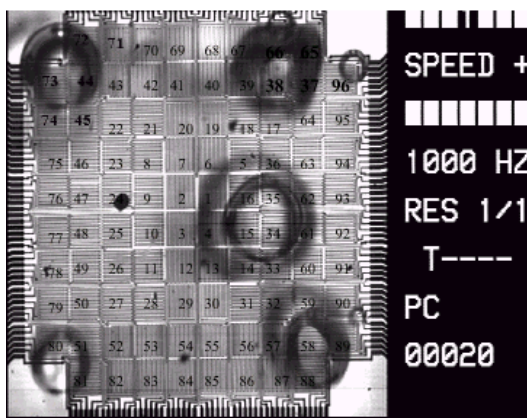


Figure 2: Photograph of boiling through the bottom of the heater array. Heater numbers were generated on picture.

The completed quartz wafer is diced into chips, each containing a single heater array. The chips are mounted on a pin-grid-array (PGA) package using epoxy adhesive and the pads on the PGA are connected to the power leads of the heater array chip using a conventional wire-bonding technique. The completed package is then mounted in a PGA socket that is connected to the control and data acquisition apparatus.

### Electronic feedback loops

The temperature of each heater in the array is kept constant by feedback circuits similar to those used in constant temperature hot-wire anemometry as shown in Figure 3. The op-amp measures the imbalance in the bridge and outputs the voltage necessary to keep the ratio  $R_H/R_1$  equal to  $R_3/R_2$ . The temperature of the heater is controlled by changing the wiper position of the digital potentiometer. The instantaneous voltage required to keep each heater at a constant temperature is measured ( $V_{out}$ ) and used to determine the heat flux from each heater element. The large  $200\text{ K}\Omega$  resistor at the top of the bridge is used to provide a small trickle current through the heater, and results in a voltage across the heater of about  $100\text{ mV}$  even when the op-amp is not regulating. Because all the heaters in the array are at the same temperature, heat conduction between adjacent heaters is negligible. There is conduction from each heater element to the surrounding quartz substrate (and ultimately to the walls of the chamber where it is dissipated by natural convection), but this can be measured and subtracted from the total power supplied to the heater element, enabling the heat transfer from the wall to the fluid to be determined.

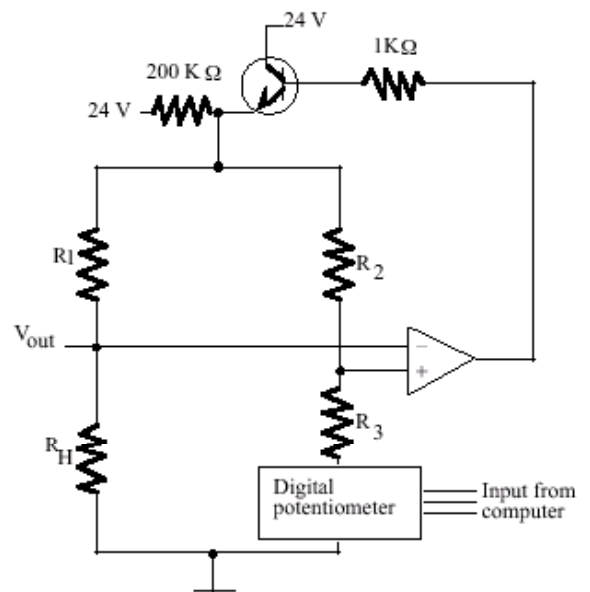


Figure 3: Schematic for heater control circuit.

The frequency response of the heaters along with the control circuit was found to be 15 kHz by measuring the time it took for the voltage across a heater to stabilize after a step change in the digital potentiometer position. Because this is much faster than the time scales typically associated with pool boiling, the heater temperatures are essentially constant throughout the bubble departure cycle.

#### Reduced gravity test rigs

Experiments in normal and microgravity have been conducted using a microscale heater array to measure time and space-resolved heat transfer. A schematic of the experimental apparatus used in the ground-based experiments is shown in Figure 4. This apparatus was supplied by NASA, and was used as a prototype for the Merte Pool Boiling Experiment that was flown aboard the space shuttle. The test fluid is FC-72 at 1 atm and measurements were performed in normal gravity at saturated conditions using an apparatus built specifically for the NASA KC-135 (Figure 5). Tests were conducted from nucleate boiling, through CHF, and into the transition boiling region.<sup>7</sup> Measurements

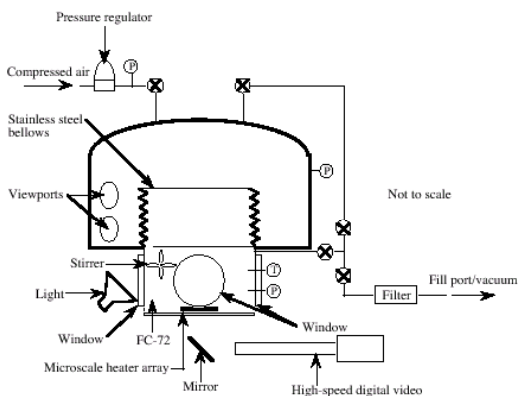


Figure 4: Diagram of test apparatus.



Figure 5: Photograph of KC-135 test apparatus.

underneath bubbles generated from a single nucleation site at two wall superheats have also been made to determine how heat is transferred by individual bubbles.<sup>8,5</sup> Measurements were also made in microgravity using the KC-135 at saturated conditions.<sup>6</sup> Finally, measurements with a highly subcooled bulk liquid were made using the Terrier-Orion sounding rocket,<sup>4</sup> see Figure 6, and subsequently in the KC-135 at other subcoolings.<sup>10</sup>



Figure 6: Terrier Orion Sounding Rocket Experiment and rocket casing.

#### RESULTS AND ANALYSIS

Typical heat flux data vs. time is shown in the top pane of Figure 7 for one of the heaters. There are periods of near-zero heater power that correspond to time intervals whereby that heater is covered by vapor and the primary heat loss is conduction through the heater substrate to the heater backside. The power that is used by the heater is primarily during periods where the heater is immersed either in liquid or a two-phase mixture of vapor and liquid. In the bottom pane, a binary boiling function is displayed.

This boiling function is “0” if vapor covers the heater, and is “1” if the heater is in contact with the liquid and boiling occurs. The heat transfer signal is conditionally sampled using the boiling function to obtain the heat flux during the period when the heater is actually heating the test liquid.

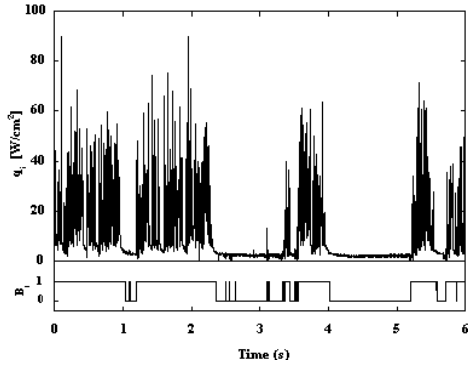


Figure 7: Typical heat flux data for a single heater in top pane, corresponding boiling function in bottom pane.

Array averaged boiling curves in earth and microgravity with the bulk fluid saturated are shown in Figure 8. It is seen that heat fluxes in microgravity are slightly larger than in earth gravity for wall superheats up to about 30 °C, but are significantly lower than in earth gravity at higher superheats. CHF in microgravity is about 30% of the value in earth gravity. The heat flux conditionally sampled on the boiling function, however, was independent of the gravity condition (Figure 9) suggesting that the small-scale bubble behavior is not affected by gravity. Heat transfer from the heater surface occurred primarily through these small bubbles, and not much heat transfer was associated with the large bubble that occasionally formed on the surface as a result of coalescence of the small bubbles.

Space-resolved heat transfer distributions on the array at three superheats with the bulk fluid subcooled by about 35 °C are shown on Figure 10. Photographic data is digitized and each heater has been color-coded according to the amount of local heat transfer that was measured with “blue” indicating negligible heat transfer and “red” indicating significant amounts of heat transfer. Low heat transfer takes place in the dry area

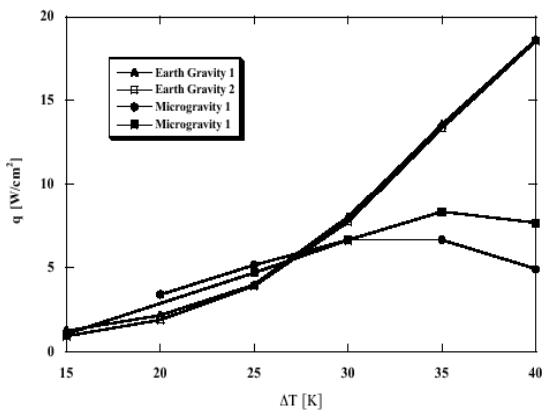


Figure 8: Array Averaged Boiling Curves.

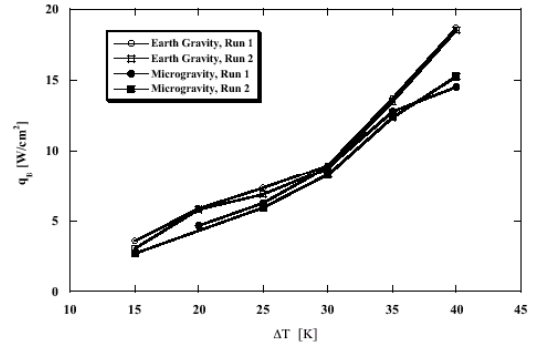


Figure 9: Array average boiling curves with boiling function applied.

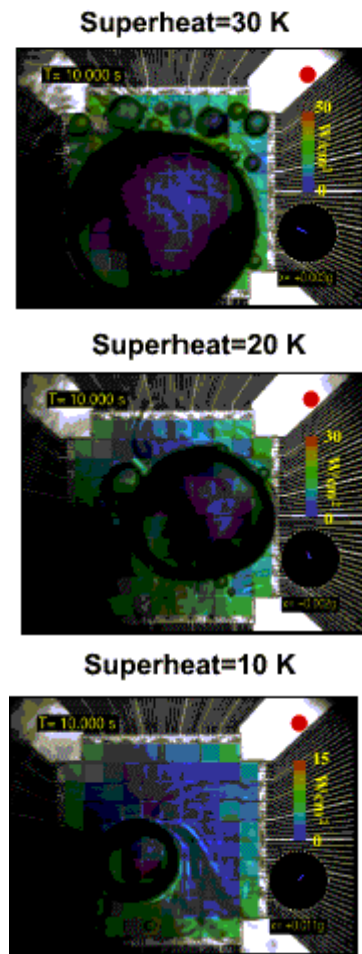


Figure 10: Colorized images of heat flux profile with regards to bubble position.

underneath the primary bubble, while large amounts of heat transfer occur during satellite bubble growth and departure as well as on the heaters cooled by convection. Occasionally, a satellite bubble grew large enough that the dry area underneath it became larger than a single heater, causing the heat flux from that heater to drop to a low value.

## PROPOSED ISS EXPERIMENT

A space-based boiling experiment using these microscale heaters has been proposed to be conducted aboard the International Space Station (ISS). The purpose of the Microheater Array Boiling Experiment (MABE) is to obtain data for the following reasons:

- to verify that behavior for the small satellite bubbles in microgravity is similar to nucleate bubble behavior in normal gravity
- to obtain a better understanding of local fluid mechanics involved with boiling in both normal and microgravity
- to examine range of applicability for using normal gravity data to predict microgravity behavior, and
- to study the role of buoyancy in boiling at varying gravity levels.

Periods of long duration, high quality microgravity are required for several reasons. First, there needs to be sufficient time to dampen out natural, or buoyancy-induced, convection that is initiated as the heater warms the test fluid. In space, heat transfer in a stagnant, single-phase fluid is by thermal conduction. While this is true aboard the KC-135 during the periods of low gravity, it is not the case during the periods of normal gravity and transitions from normal through 1.8 g's to microgravity. Because of small changes in the liquid density due to temperature dependence of density, natural convection occurs within the test chamber. This flow eventually stops in low gravity, but the time that it takes depends on the initial rate, the size of the chamber and the fluid viscosity. In addition, the quality of the low gravity period (magnitude and direction) aboard the KC-135 is poor, and has been measured to be as high as 0.02 g's due to such factors as weather-induced turbulence and pilot proficiency. These excursions are sufficient to cause bubbles, especially the large primary bubbles, to lift off and prematurely depart the heater surface.

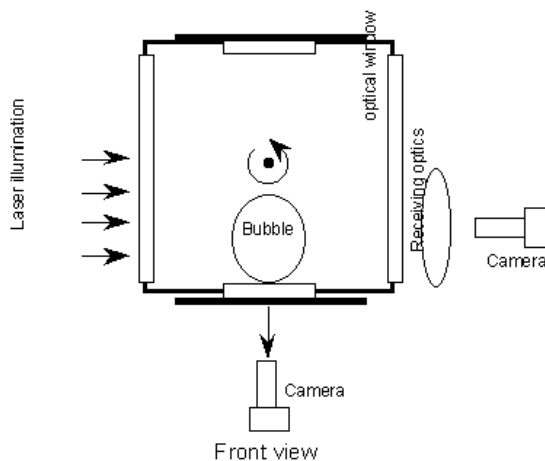


**Figure 12: System schematic of microheater array boiling experiment.**

A very limited number of test points were conducted aboard a Terrier-Orion sounding rocket. The quality of microgravity was exceptional, on the order of less than  $3 \mu\text{g}'\text{s}$ . The period of low gravity was approximately 200 s permitting the boiling behavior at multiple wall temperatures to be observed. However, given the size of the projected test matrix, see Table 1, it is not cost-effective to use multiple sounding rocket launches to complete the program.

The experiment is therefore being baselined aboard the ISS in the Microgravity Science Glovebox (MSG). A conceptual layout is shown in Figure 11 and a schematic is shown in Figure 12. The experiment will use FC-72 as the test fluid and consists of several features including the following:

1. 2 by 2 cm heater and a 7 by 7 cm array
2. Test chamber with pressure and temperature control
3. High speed video system
4. Standard Video system
5. Temperature field measurement system.

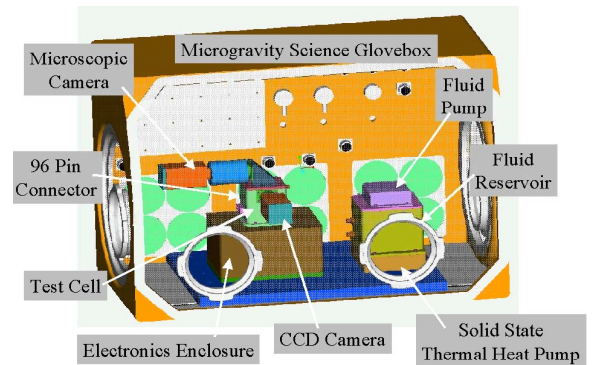


**Figure 11: Conceptual layout of microheater array boiling experiment in MSG.**

**Table 1: Proposed test matrix.**

Conditions No.	(mm)	Temperature (°C)	(atm), T <sub>sat</sub> (°C)	Active Heaters	Heater Temperatures (°C)
1	2.7	50	1.0, 56	96,64, 36	110, 105, 100, 95, 90, 85, 80, 75, 70, 65
2	2.7	50	1.5, 69	96,64, 36	110, 105, 100, 95, 90, 85, 80, 75
3	2.7	50	2.0, 79	96,64, 36	110, 105, 100, 95, 90, 85
4	2.7	35	1.0, 56	96,64, 36	110, 105, 100, 95, 90, 85, 80, 75, 70, 65
5	2.7	35	1.5, 69	96,64, 36	110, 105, 100, 95, 90, 85, 80, 75
6	2.7	35	2.0, 79	96,64, 36	110, 105, 100, 95, 90, 85
7	2.7	20	1.0, 56	96,64, 36	110, 105, 100, 95, 90, 85, 80, 75, 70, 65
8	2.7	20	1.5, 69	96,64, 36	110, 105, 100, 95, 90, 85, 80, 75
9	2.7	20	2.0, 79	96,64, 36	110, 105, 100, 95, 90, 85
10	7	50	1.0, 56	96,64, 36	110, 105, 100, 95, 90, 85, 80, 75, 70, 65
11	7	50	1.5, 69	96,64, 36	110, 105, 100, 95, 90, 85, 80, 75
12	7	50	2.0, 79	96,64, 36	110, 105, 100, 95, 90, 85
13	7	35	1.0, 56	96,64, 36	110, 105, 100, 95, 90, 85, 80, 75, 70, 65
14	7	35	1.5, 69	96,64, 36	110, 105, 100, 95, 90, 85, 80, 75
15	7	35	2.0, 79	96,64, 36	110, 105, 100, 95, 90, 85
16	7	20	1.0, 56	96,64, 36	110, 105, 100, 95, 90, 85, 80, 75, 70, 65
17	7	20	1.5, 69	96,64, 36	110, 105, 100, 95, 90, 85, 80, 75
18	7	20	2.0, 79	96,64, 36	110, 105, 100, 95, 90, 85

It is anticipated that the astronaut involvement will be primarily for the assembly and removal of the experiment after its completion. After the first half of test conditions have been completed, the astronaut will switch connectors and reposition either the test chamber or camera and optics in order to change from the 2 by 2 cm array to the 7 by 7 cm array.

Experiment control will be automated and controlled by the data acquisition system. Owing to the large amount of data that will be collected by the video cameras, especially the high speed video camera and the heater arrays (96 heaters at 500 Hz each), all data will be stored onboard the experiment. A small representative amount will be telemetered to the Principal Investigator and his science team to make minor modifications to the test matrix in order to optimize the test matrix.

The data and video will be synchronized in order to correlate the position of vapor and liquid with respect to local heat flux and acceleration measurements. The liquid temperature profile will also be synchronized with the position of the side view camera in order to distinguish between interferometric fringes and the bubble interface.

#### SUMMARY

MABE promises to deliver a wealth of data with unique qualities including time and spatial resolved heat flux in relation to bubble position throughout the boiling curve. It is anticipated that this data shall not only validate the premise that all heaters in microgravity behave like small heaters in normal gravity, but shall provide significant insight into the fluid dynamics at the heater surface.

## REFERENCES

1. Fritz, W. (1935) "Berechnungen des Maximalvolumens von Dampfblasen," *Phys. Z.*, Vol. 36, pp. 379–384.
2. Han, C.Y. and Griffith, P. (1965), "The Mechanism of Heat Transfer in Nucleate Pool Boiling—Part I," *Int. J. of Heat and Mass Transfer*, Vol. 8, pp. 887.
3. Haramura, Y. and Katto, Y.A. (1983) "A new Hydrodynamic Model of Critical Heat Flux Applicable Widely to Both Pool and Forced Convection Boiling on Submerged Bodies in Saturated Liquids," *Int. J. of Heat and Mass Transfer*, Vol. 26, pp. 389–399.
4. Kim, J., Benton, J.F., and Kucner, R. (2000), "Subcooled Pool Boiling Heat Transfer Mechanisms in Microgravity: Terrier-Improved Orion Sounding Rocket Experiment," NASA/CR—2000-210570.
5. Kim, J., Demiray, F., and Yaddanapudi, N. (2000) "Saturated Pool Boiling Mechanisms During Single Bubble Heat Transfer: Comparison at Two Temperatures," *Proceedings of the 2000 ASME IMECE, Orlando, FL.*
6. Kim, J., Yaddanapudi, N., and Mullen, J.D., "Heat Transfer Behavior on Small Horizontal Heaters During Saturated Pool Boiling of FC-72 in Microgravity," accepted for publication in *Microgravity Science and Application*, 2000.
7. Rule and Kim, J., "Heat Transfer Behavior on Small Horizontal Heaters During Pool Boiling of FC-72," *Journal of Heat Transfer*, Vol. 121, No. 2, May 1999, pp. 386–393.
8. Yaddanapudi, N. and Kim, J., (2001) "Single Bubble Heat Transfer in Saturated Pool Boiling of FC-72," Accepted for publication in *Multiphase Science and Technology*.
9. Zuber, N. (1959) "Hydrodynamic Aspects of Boiling Heat Transfer," AEC Report AECU-4439, Physics and Mathematics.
10. Kim, J., Benton, J.F., and Wisniewski, D., "Microgravity Pool Boiling Heat Transfer: Effects of Gravity and Subcooling Level," 2001 Engineering Foundation Conference on Microgravity Transport Processes in Fluid, Thermal, Biological, and Materials Science Conference II, September 30–October 5, 2001, Banff, Canada.

# REPORT DOCUMENTATION PAGE

*Form Approved*  
*OMB No. 0704-0188*

Public reporting burden for this collection of information is estimated to average 1 hour per response, including the time for reviewing instructions, searching existing data sources, gathering and maintaining the data needed, and completing and reviewing the collection of information. Send comments regarding this burden estimate or any other aspect of this collection of information, including suggestions for reducing this burden, to Washington Headquarters Services, Directorate for Information Operations and Reports, 1215 Jefferson Davis Highway, Suite 1204, Arlington, VA 22202-4302, and to the Office of Management and Budget, Paperwork Reduction Project (0704-0188), Washington, DC 20503.

<b>1. AGENCY USE ONLY</b> ( <i>Leave blank</i> )		<b>2. REPORT DATE</b> January 2002	<b>3. REPORT TYPE AND DATES COVERED</b> Technical Memorandum	
<b>4. TITLE AND SUBTITLE</b>  Microheater Array Boiling Experiment			<b>5. FUNDING NUMBERS</b>  WU-101-43-0A-00	
<b>6. AUTHOR(S)</b>  Jungho Kim, John McQuillen, and Joe Balombin				
<b>7. PERFORMING ORGANIZATION NAME(S) AND ADDRESS(ES)</b>  National Aeronautics and Space Administration John H. Glenn Research Center at Lewis Field Cleveland, Ohio 44135-3191			<b>8. PERFORMING ORGANIZATION REPORT NUMBER</b>  E-13032	
<b>9. SPONSORING/MONITORING AGENCY NAME(S) AND ADDRESS(ES)</b>  National Aeronautics and Space Administration Washington, DC 20546-0001			<b>10. SPONSORING/MONITORING AGENCY REPORT NUMBER</b>  NASA TM-2002-211167 AIAA-2001-5116	
<b>11. SUPPLEMENTARY NOTES</b>  Prepared for the International Space Station Utilization-2001 sponsored by the American Institute of Aeronautics and Astronautics, Cape Canaveral, Florida, October 15-18, 2001. Jungho Kim, University of Maryland, College Park, Maryland 20742; John McQuillen and Joe Balombin, NASA Glenn Research Center. Responsible person, John McQuillen, organization code 6712, 216-433-2876.				
<b>12a. DISTRIBUTION/AVAILABILITY STATEMENT</b>  Unclassified - Unlimited Subject Category: 34  Available electronically at <a href="http://gltrs.grc.nasa.gov/GLTRS">http://gltrs.grc.nasa.gov/GLTRS</a> This publication is available from the NASA Center for AeroSpace Information, 301-621-0390.			<b>12b. DISTRIBUTION CODE</b>	
<b>13. ABSTRACT</b> ( <i>Maximum 200 words</i> )  By conducting pool boiling tests in microgravity, the effect of buoyancy on the overall boiling process and the relative magnitude of other phenomena can be assessed. Data from KC-135 and sounding rocket experiments indicate little effect of gravity on boiling heat transfer at wall superheats below 25 °C, despite vast differences in bubble behavior between gravity levels. In microgravity, a large primary bubble, surrounded by smaller satellite bubbles, moved over the surface, occasionally causing nucleation. Once formed, the primary bubble size remained constant for a given superheat, indicating evaporation at the bubble base is balanced with condensation on the bubble cap. The primary bubble's size increased with wall superheat. Most heaters under the primary bubble had low heat transfer rates, suggesting liquid dryout. Strong Marangoni convection developed in microgravity, forming a "jet" into the bulk liquid that forced the bubble onto the heater. An experiment is being designed for the Microgravity Science Glovebox. This experiment uses two 96 element microheater arrays, 2.7 and 7.0 mm in size. These heaters are individually controlled to operate at a constant temperature, measuring local heat fluxes as a function of time and space. Most boiling experiments operate at constant wall heat flux with larger heaters, allowing only time and space-averaged measurements. Each heater is about the bubble departure size in normal gravity, but significantly smaller than the bubble departure size in reduced gravity.				
<b>14. SUBJECT TERMS</b>  Microgravity; Boiling; Two-phase flow			<b>15. NUMBER OF PAGES</b> 14	
			<b>16. PRICE CODE</b>	
<b>17. SECURITY CLASSIFICATION OF REPORT</b> Unclassified	<b>18. SECURITY CLASSIFICATION OF THIS PAGE</b> Unclassified	<b>19. SECURITY CLASSIFICATION OF ABSTRACT</b> Unclassified	<b>20. LIMITATION OF ABSTRACT</b>	